Developmental Cell *19*

Supplemental Information

Osteoblast Precursors, but Not Mature Osteoblasts, Move into Developing and Fractured Bones along with Invading Blood Vessels

Christa Maes, Tatsuya Kobayashi, Martin K. Selig, Sophie Torrekens, Sanford I. Roth, Susan Mackem, Geert Carmeliet, and Henry M. Kronenberg

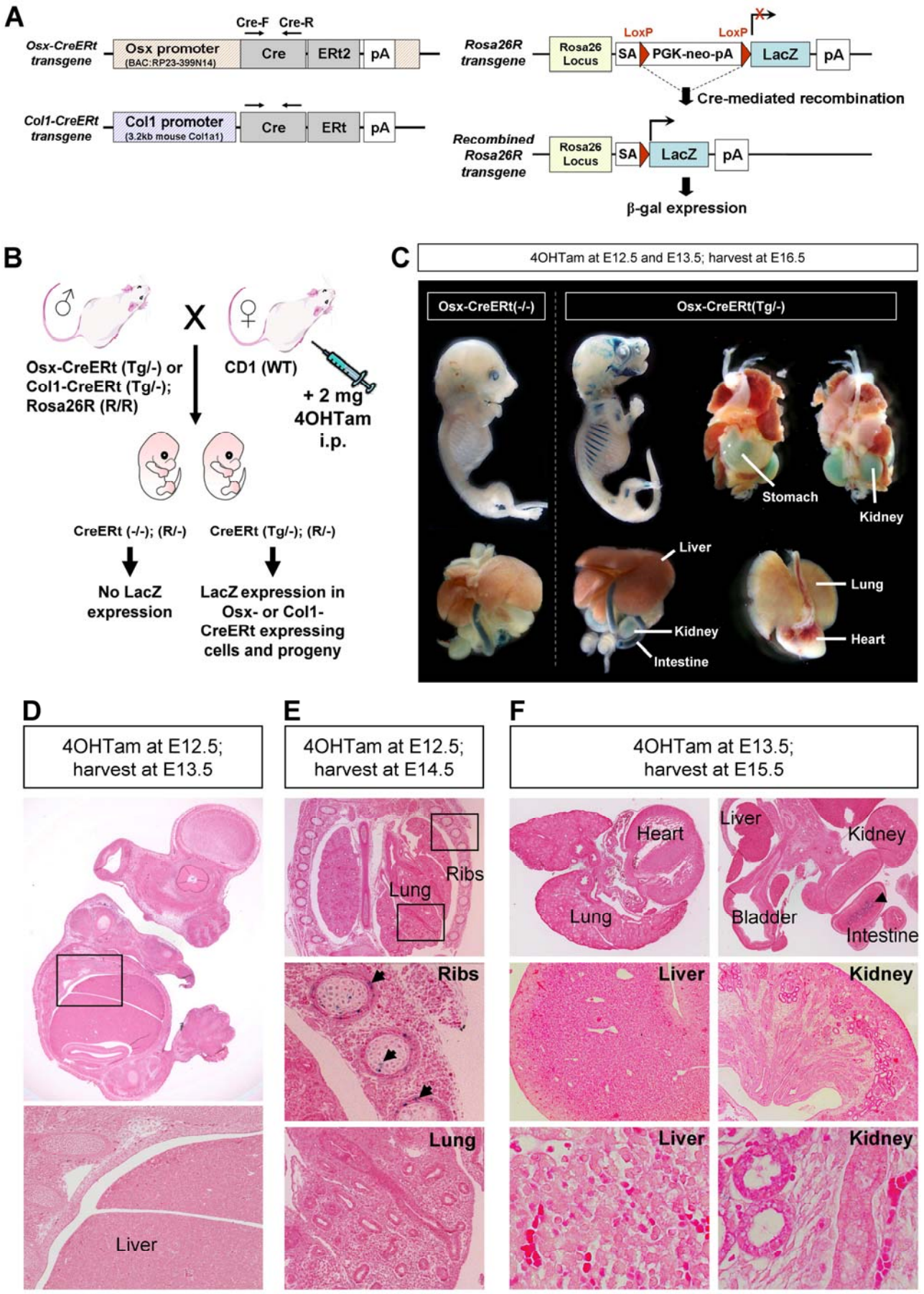

Figure S1. Generation and characterization of transgenic mice expressing CreERt in osteoblast lineage cells (related to Figure 1)

(A) Schematic representation of the transgenes used in this study. Osx-CreERt2 and Col1-CreERt constructs (left) were generated by cloning the Cre-ERt(2) fusion protein cDNA and downstream poly-A element (pA) into a BAC containing the *Osterix* (*Sp7*) (*Osx*) gene promoter or behind a 3.2 kb fragment of the mouse type I collagen (*collagen Iα1*, abbreviated to *Col1*) regulatory sequences. Arrows indicate the positions of the forward (Cre-F) and reverse (Cre-R) primers for genotyping the resultant transgenic mice. Each of the lines was crossed to Rosa26R reporter mice that contain a LacZ transgene downstream of a floxed stop-cassette at the ubiquitously expressed Rosa26 locus. The recombination of the transgene results in constitutive LacZ/β-galactosidase (β-gal) expression (right). SA, splice acceptor.

(B) Outline of the experimental design. The Rosa26R transgene was crossed to homozygosity into the Osx- and Col1-CreERt lines. Male Osx- or Col1-CreERt(Tg/-);Rosa26R(R/R) mice were timed mated to non-transgenic CD1 females. Pregnant females received 2 mg of 4OHTam by i.p. injection at specific time points to activate CreERt in the transgenic embryos, all carrying one Rosa26R allele (not further designated). Subsequent X-gal staining (blue) of the embryonic progeny identified cells that had undergone CreERt-mediated recombination of the Rosa26R transgene and the descendants thereof, as these cells expressed LacZ. Osx- or Col1-CreERt(-/-);Rosa26R(R/-) littermates served as negative controls. Of note, 2 mg 4OHTam was effective and nontoxic in most females, although occasionally embryos were lost. Injection of 4OHTam to the mother did not adversely affect embryonic growth and organogenesis, as the pups had normal body weights (not shown) and overall appearance at all stages, and the temporal or morphological characteristics of skeletal development seemed unaffected (as seen throughout this work).

(C) Whole-mount views of the skeleton and organs of E16.5 Osx-CreERt(-/-) and Osx-CreERt(Tg/-) littermates that were exposed to 4OHTam twice, at E12.5 and at E13.5, and stained with X-gal overnight. Only Osx-CreERt(Tg/-) embryos show blue staining throughout the bone regions of the skeleton. Non-skeletal tissues do not stain blue in either genotype, with the exception of non-specific vague blue coloration often associated with the luminal side of the stomach, kidney, and most notably the intestine.

(D-F) Histological examination of non-skeletal tissues of Osx-CreERt(Tg/-) embryos sacrificed 1-2 days after exposure to 4OHTam at E12.5 or E13.5. Except for the X-gal staining associated with skeletal elements (arrows in (E)), no Osx-CreERt activation is detected in sagittal sections throughout E13.5 embryos (D, boxed area magnified below), coronal sections through the chest at E14.5 (E, magnified views of ribs and lung in lower panels), and sections of internal organs harvested at E15.5 (F, increasing magnifications from top to bottom). These data support the absence of Osx-CreERt transgene expression in non-skeletal locations.

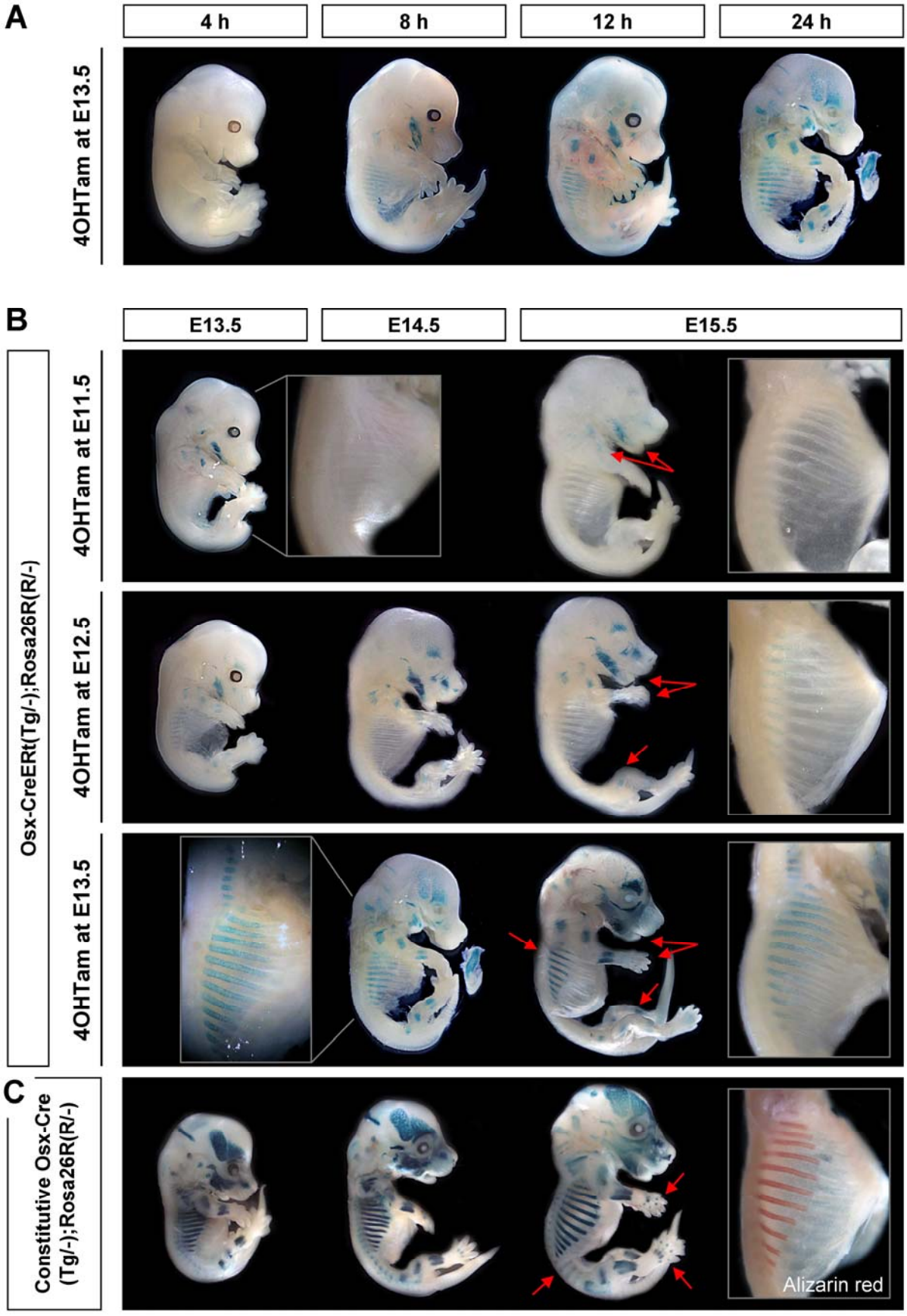

Figure S2. Kinetics of 4OHTam-induced, Osx-CreERt-mediated activation of the Rosa26R reporter transgene: fast induction and complete reversal (related to Figure 2)

(A-B) Lineage tracing requires tightly controlled induction of recombination within a narrow time window of action. To assess the kinetics of the system, we defined (A) the minimal time required for visual induction of LacZ activity, and (B) the end point of the labeling time window following 4OHTam injection, defining the start of the actual cell tracing (chase) period. As shown here, X-gal staining became detectable as early as 8 h after 4OHTam injection and its pattern of distribution remained similar thereafter.

(A) A set of females, mated to Osx-CreERt(Tg/-) mice, was pulsed with 4OHTam at E13.5 and the offspring was retrieved at varying time points thereafter. Overnight X-gal staining of whole embryos is shown. When harvested at 4 h post-injection, Osx-CreERt(Tg/-) embryos did not show visible LacZ induction and/or accumulation. From 8 h onwards, blue staining became readily detectable in the skeleton and intensified over time. The signal was observed in the mandible (shown separated from the 24 h sample, right), calvaria, ribs, and in the limb bones excluding the autopod.

(B) Pulse-chase strategy using 24 h intervals providing evidence that the induction of Osx-CreERt-activity and the resultant Rosa26R recombination finished within less than a day after 4OHTam-injection. We systematically varied the times of 4OHTam injection (between E10.5 and E13.5) and embryo retrieval (at subsequent days up to E16.5) (not all time points shown), revealing that the specific combination of skeletal elements that stained blue was determined exclusively by the time of 4OHTam injection (i.e. by the developmental progress of the various skeletal elements at that time), not by the age of the embryo at sacrifice. Top: Injection of 4OHTam at E11.5 induced X-gal staining exclusively in the mandibles and proximal forelimbs, irrespective of the time of sacrifice (E13.5 or E15.5), indicating that no additional Rosa26R recombination had taken place beyond E13.5. Insets, magnified views of the thorax (after removal of the forelimbs). Middle: Embryos that received 4OHTam at E12.5 and were sacrificed at E13.5, E14.5 or E15.5, all displayed the same staining pattern. Skull bones, forelimbs and hind limbs contain blue domains, while X-gal staining in the ribs is minimal. Bottom: Embryos exposed to 4OHTam at E13.5 and sacrificed at E14.5 or E15.5 additionally displayed extensive labeling of the ribs, in contrast to embryos that received 4OHTam 24 or 48 h earlier in development (compare the columns). The differential staining patterns observed in embryos collected at the same age but pulsed with 24 h time intervals (e.g. red arrows) prove that functional CreERt-activation is limited to a maximum of 24 h in vivo. For example, hind limbs became labeled when 4OHTam was given at E12.5 but not when injected at E11.5. Presumably, in the latter case the 4OHTam concentration was already too low when Osx-CreERt became expressed. The same activation window (<24 h) was operative for the Col1-CreERt line (data not shown). Of note, these experiments revealed that Osx-CreERt-expressing cells in the bones of the limbs, which we wished to study in detail, could be genetically labeled from E12.5 onwards.

(C) X-gal staining of embryos expressing a constitutive Osx-Cre:GFP transgene (Rodda and McMahon, 2006), engineered using the same Osx-promoter containing BAC fragment, and mated to Rosa26R reporter mice. At all stages (E13.5, E14.5 and E15.5 shown), the staining pattern correlates but is more extensive and intense compared with induced Osx-CreERt embryos (compare vertically with (B)) confirming the tight induction-dependent activity and full closure of the Osx-CreERt transgene. Arrows (in E15.5 images) point out skeletal elements that start to express Osx-Cre:GFP at E14.5-E15.5 and do not become labeled in Osx-CreERt embryos given 4OHTam at E13.5, again confirming the less-than-24 h induction window.

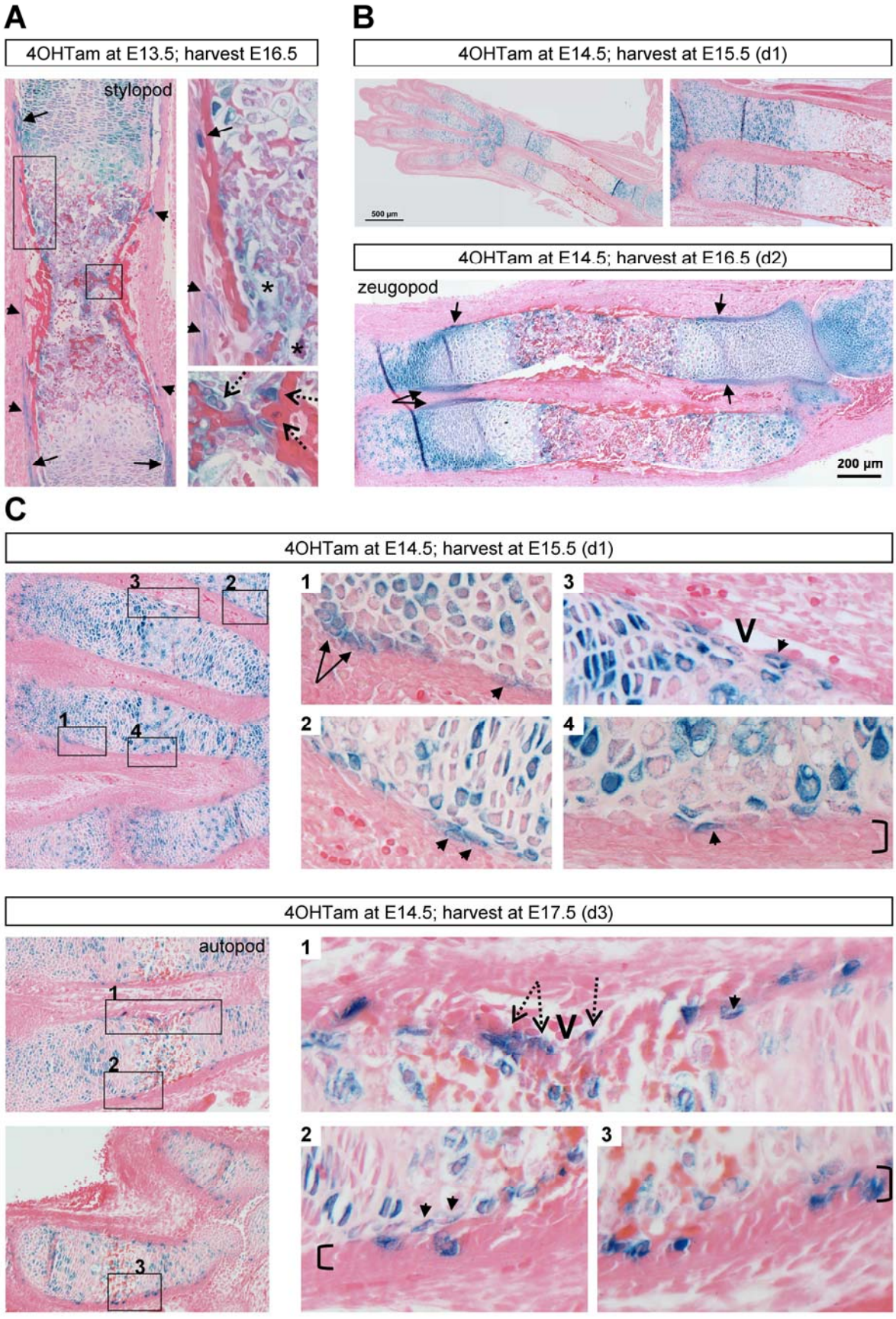

Figure S3. Collagen type II (Col2)-expressing cells early in endochondral bone development include chondro-perichondrial progenitors that give rise to both chondrocytes and osteoblasts (related to Figure 3)

(A-C) Early activation of Col2-CreERt in cartilaginous bone templates (by injecting 4OHTam well before the start of primary ossification) led to X-gal staining in chondrocytes as well as perichondrial/periosteal cells and their osteoblastic descendants within a 3-day-tracing period. This was observed in the most proximal (stylopod) elements of the limbs when injecting 4OHTam at E13.5 (A) and in the more distal bones (that are less advanced in development) even when 4OHTam was given at E14.5 (B and C).

(**A**) Section through the humerus of a Col2-CreERt(Tg/-) embryo exposed to 4OHTam at E13.5 and sacrificed at E16.5. Col2/LacZ+ cells are seen in the perichondrium/periosteum (arrows and arrowheads, respectively), and in cells with osteoblast morphology on bone surfaces (dashed arrows in magnification). It is currently unclear whether the blue staining associated with the lining and lumen of blood vessels (asterisks) is cell-specific or reflective of dye released following cartilage resorption.

(**B**) Administration of 4OHTam to Col2-CreERt(Tg/-) mice at E14.5 followed by X-gal staining one day later (d1, upper panels) indicates that in the lower forelimb the labeling is mostly restricted to chondrocytes (left). By d2 post-injection, staining is marked additionally in the perichondrial regions (arrows) and concomitantly, Col2/LacZ+ cells are observed inside the bone shaft (particularly near the endosteal surfaces). The origin of these cells (chondrocytic or perichondrial) is therefore uncertain.

(**C**) Cell tracing in the cartilaginous autopod at these stages, revealing that Col2-CreERt-expressing cells early in development can give rise to perichondrial cells and attain a morphology and positioning consistent with properties of osteoblast precursors. Upper panels: overview (left) and magnifications of the boxed regions (right) show blue cells at the poorly delineated transition zone between the cartilage and perichondrium (arrows in (1)) and cells at the periphery of the cartilage attaining a transversal orientation to the more central growth chondrocytes (arrowheads in (2)). Closer to the diaphysis, such cells (arrowheads) locate to the perichondrial side where blood vessels (V in (3)) accumulate and the cambium layer of cuboidal cells develops (bracket in 4). Lower panels: by d3, Col2/LacZ+ cells populate the perichondrium, appearing at the mid-diaphyseal vascular pre-invasion site (dashed arrows in (1)) and in the cambium layer (brackets in (2) and (3)) resembling osteoblast precursors. Transversal oriented ‘borderline chondrocytes’ (arrowheads) are seen, apparently escaping hypertrophic differentiation.

These lineage tracing results indicate that Col2-expressing cells labeled at *early* stages of endochondral bone development contribute to a population of chondro-perichondrial progenitors. When cells follow this pathway prior to primary ossification, their progeny include chondrocytes as well as osteoblast lineage cells in the bone collar and inside the bone subsequently. These findings are supplemental to Figure 3, in which tracing of growth cartilage chondrocytes labeled at an *advanced* developmental stage indicates that terminally matured chondrocytes are unlikely to contribute significantly to the trabecular osteoblasts in the central metaphyseal regions.

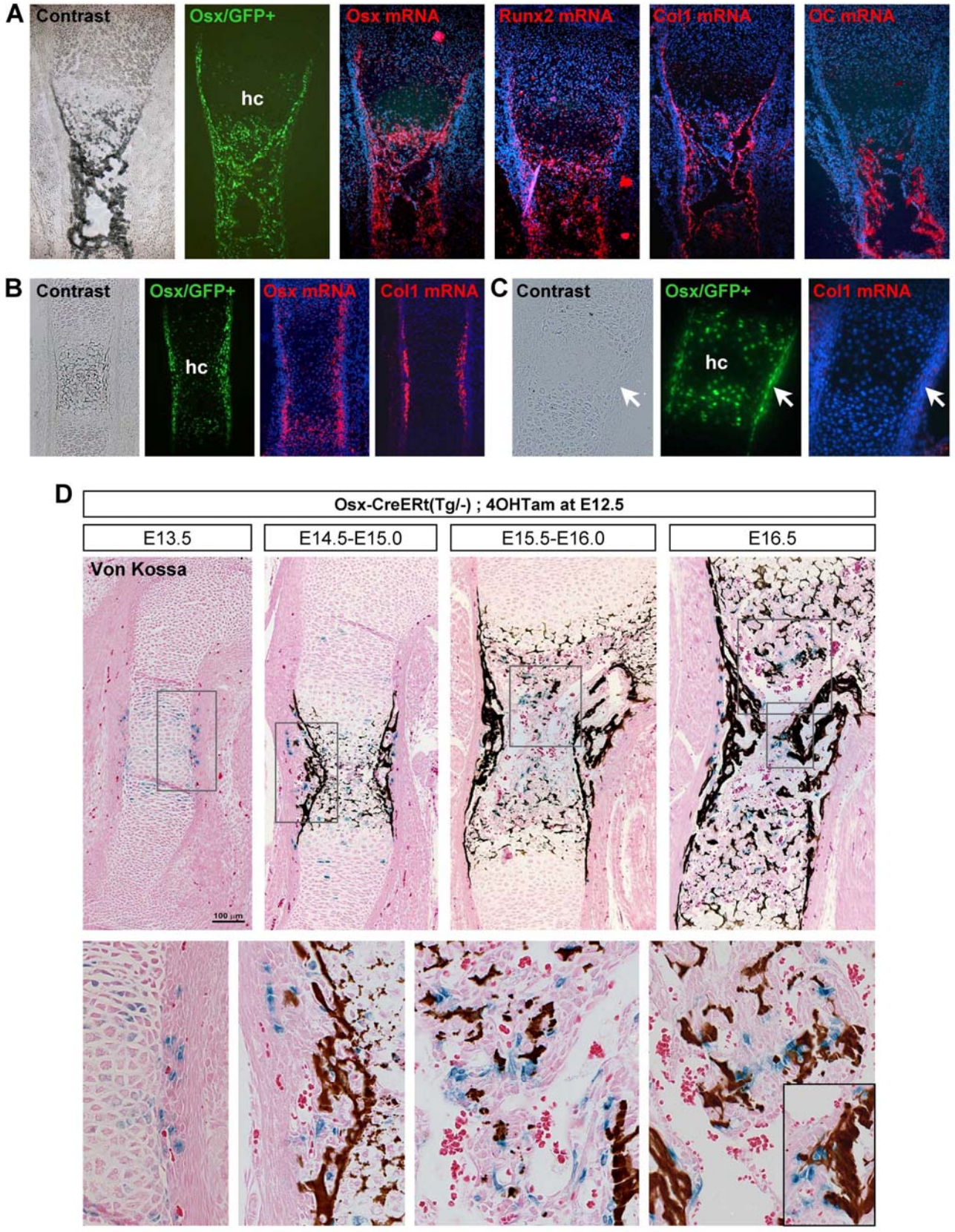

Figure S4. Earlier activation of Osx-CreERt compared with Col1-CreERt in development correlates with the differential timing of activation of the endogenous *Osx*- and *Col1*-gene promoters (related to Figure 4)

To assess the relevance of the transgenic models employed in this study we compared the relative timing and patterns of *Osx*- and *Col1*-gene promoter driven CreERt-mediated LacZ-labeling with the expression of the respective endogenous genes and of the early and late osteoblast differentiation markers Runx2 and osteocalcin, as well as with the expression of an independently generated Osx-Cre:GFP transgene in mice (allowing co-localization studies with the GFP signal).

(**A-C**) In situ hybridization (ISH) of sets of consecutive sections through the hind limbs of Osx-Cre:GFP embryos at E16.5 with probes detecting Osx, Runx2, Col1, and/or osteocalcin (OC) mRNAs (shown as red signals on Hoechst nuclear counterstain). Contrast light image and GFP fluorescent view are shown on the left. hc, hypertrophic cartilage. The proximal-to-distal sequence in the developmental timing of the various bones of the limbs permits analysis at stepwise stages in the tibia (A, primary ossification center established; section containing (top-to-bottom) growth cartilage, trabecular region, and cortical bone is shown), metatarsals (B, calcified hypertrophic cartilage stage (visible on contrast image), just prior to initial invasion), and phalanges (C, less advanced cartilaginous stage (non-calcified, see contrast image). At all developmental stages, the Osx/GFP+ signal correlated tightly with the expression of endogenous Osx mRNA, corresponding closely to the pattern of Runx2 expression in the bone ((A-C) and data not shown).

(**A**) The distribution of Col1 mRNA expression was similar but (subtly) less broad throughout the developing tibia at E16.5 (also see further, Figure S5B), while the expression of the fully mature osteoblast marker osteocalcin was more restricted, primarily to the cortical bone. Of note, injection of 4OHTam at E15.5 or E16.5 in our CreERt models generated mosaic Osx/LacZ+ and Col1/LacZ+ cell labeling patterns corresponding to the expression patterns of the respective endogenous genes as seen here (data not shown).

(**B**) Perichondrial cells around non-invaded calcified hypertrophic cartilage expressed both Osx and Col1 mRNAs, correlating with the labeling patterns of Osx-CreERt and Col1-CreERt mice that received 4OHTam at E13.5 (see Figure 2A).

(**C**) At an early developmental stage, preceding cartilage calcification and bone collar mineralization, perichondrial cells expressing Osx/GFP and Osx mRNA (not shown) appear prior to the detection of Col1 mRNA expression (arrows). In parallel, injecting 4OHTam at E12.5 allowed the labeling of perichondrial Osx/LacZ+ cells but not Col1/LacZ+ cells (see (D) and Figure 4).

(**D**) Combined X-gal/Von Kossa staining of humerus sections illustrating the pulse-chase approach used to follow Osx/LacZ+ cells labeled early in development, by 4OHTam-injection at E12.5, over subsequent 1-day-intervals. Note that in the E13.5 cartilaginous humerus, labeled Osx/LacZ+ cells appear, as expected, prior to mineralization (absence of black deposits), corresponding to the developmental stage shown in (C). Lower images, magnifications of boxed areas. Scale bar, 100 μm.

Altogether, these data indicate that the differential timing of activation of the *Osx*- and *Col1*-gene promoters correlates with the potential to selectively label the earliest Osx-CreERt-expressing osteoblast precursor cells.

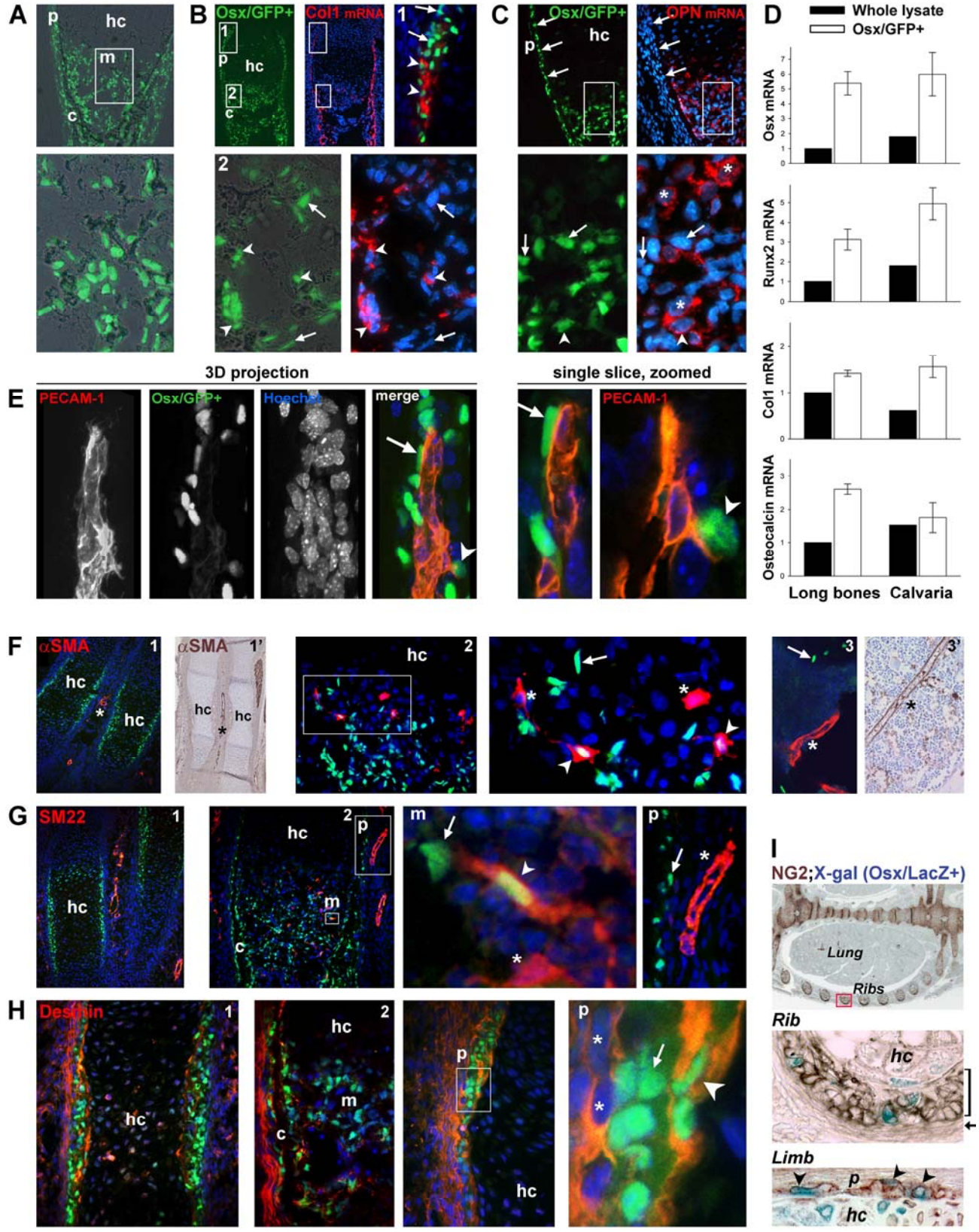

Figure S5. Osx-expressing cell populations include cells expressing osteoblastic genes, angiogenic stimuli and pericyte markers (related to Figure 5)

(A-I) Molecular characterization of Osx-expressing cells. Abbreviations used throughout this figure: hc, hypertrophic cartilage; p, perichondrium; m, metaphysis; c, cortex. Markers: arrows, Osx/GFP+

cells not expressing the molecular staining target; arrowheads, double positive cells; asterisks, Osx/GFP-negative cells expressing the molecule of interest.

(A) Overlay of contrast and GFP images of E16.5 Osx-Cre:GFP tibia sections showing that many, but not all, of the Osx/GFP+ cells inside the primary ossification center localized to the trabecular bone surface. The indicated boxed area is magnified below.

(B) Fluorescent ISH with DIG-labeled Col1 probes detected by cellular anti-DIG antibody staining (red signal) in E16.5 Osx-Cre:GFP tibias, revealing that many but not all Osx/GFP+ cells expressed endogenous Col1 mRNA. Top left, overview images of the section with landmarks to the tissue outline and magnified areas (box 1, periosteum (magnified on the right); box 2, metaphysis/endosteum (magnified below)). Each area was captured before the ISH procedure to visualize the Osx/GFP signal (shown overlaid on contrast background) and afterwards, detecting the red mRNA signal (and blue Hoechst-stained nuclei). Images were location-matched and are shown side-by-side (with corresponding arrow(head)s indicators), except for the magnified view of box 1 (periosteum) where the three channels (RGB) were merged into a single image.

(C) Similar ISH analysis for the combined detection of Osx-expressing cells (Osx/GFP+) and osteopontin (OPN) (red).

(D) qRT-PCR analysis of Osx, Runx2, Col1, and osteocalcin expression in Osx/GFP+ FACS-sorted cell populations (mean ± SEM; n=4) derived from collagenase-digested long bones (left set of bars) or calvaria (right set of bars) from newborn Osx-Cre:GFP mice. Control samples represent similarly treated digests of Osx-Cre:GFP-negative littermates. Note strong enrichment in transcripts of the early precursor markers Osx and Runx2 (~3-5-fold), and more moderate enrichment in mRNAs for the mature osteoblast markers Col1 and osteocalcin.

(E) Confocal microscopy analysis of PECAM-1 stained vibratome sections of the tibia of adult Osx-Cre:GFP mice. Osx/GFP+ cells could regularly be detected in close vicinity of some of the metaphyseal blood vessels. Images show the red (PECAM-1), green (Osx/GFP) and blue (Hoechst) channels of a 3D projection of a blood vessel, separately and merged as indicated. Single confocal slices zooming in on the indicated cells (arrow and arrowhead corresponding to those in the 3D image), revealing their immediate juxtaposition to the endothelium.

(F-I) Expression pattern of the pericyte markers (F) αSMA, (G) SM22, (H) desmin, and (I) NG2 in endochondral bones as detected by fluorescent (red signal on Osx/GFP+ samples) or light (DAB, brown) IHC. Bones were examined at the early cartilaginous stage in E14.5 limbs or E16.5 metatarsals (panels marked ‘1’), in E16.5 tibia sections (‘2’), or postnatal (‘3’). Marks are as outlined above unless indicated otherwise. (F) (1, 1’), Before primary ossification, αSMA is detected only in skeletal muscle and blood vessels outside the bones (asterisk, large vessel running between the radius and ulna) and not in the cartilage and perichondrium. (2, box magnified on the right), Only some isolated αSMA+ cells were detected inside the metaphysis of E16.5 tibia, a subset of which was Osx/GFP+. PECAM-1 staining on subsequent sections confirmed that the blood vessels of embryonic bones are not covered by classical, αSMA+, pericytes (not shown). (3, 3’), Only rare large blood vessel in the marrow cavity of postnatal bones (3-month-old and postnatal day 6 shown) are fully covered by αSMA+ pericytes; this vessel-associated αSMA+ staining does not coincide with Osx/GFP-expression. Similarly, αSMA+ pericytes in internal organs (lung, heart, liver and kidney) were all Osx/GFP-negative or Osx/LacZ-negative (data not shown). (G) SM22 detection on similar sections reveals a similar pattern as described for αSMA. (H) Desmin expression is detected in perichondrial cells either or not Osx/GFP+, but does not show a pattern reflecting the vascular

pattern in bone. (I) IHC for NG2 (brown) on sections through the thorax, cartilaginous ribs (magnified from red box in top image), and limbs (bottom) of E14.5 Osx-CreERt(Tg/-) mice exposed to 4OHTam at E12.5 and stained with X-gal. Membranous NG2 is associated with the osteoblastic cambium layer (bracket) of the perichondrium and not with the outer fibrous layer (arrow). Perichondrial Osx/LacZ+ cells express NG2 (arrowheads).

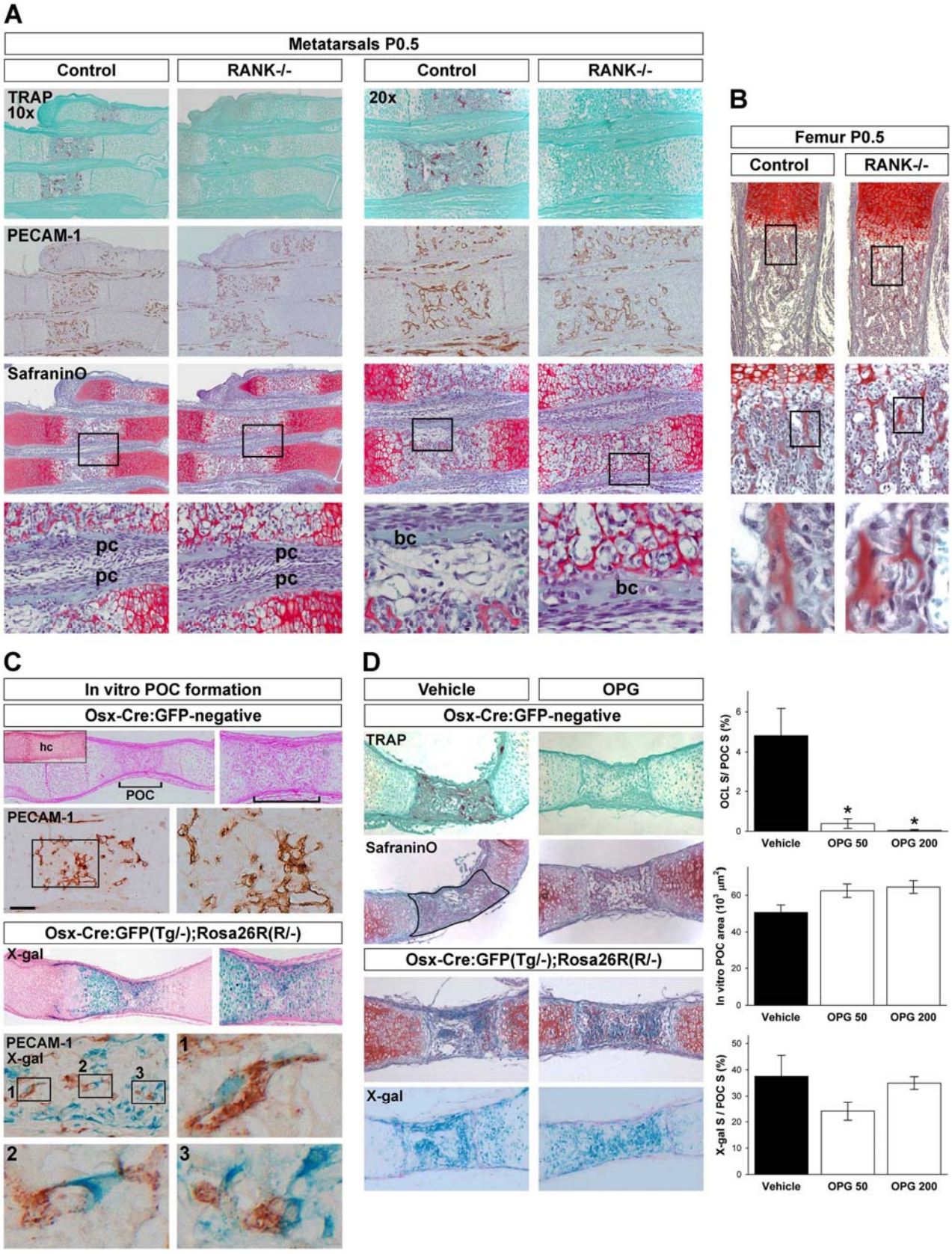

Figure S6. Lack of osteoclasts does not preclude initial vascular invasion of cartilage and primary ossification center formation in vitro and in vivo (related to Figure 6)

(A) Histology of the metatarsals of newborn mice lacking RANK (RANK-/-) and of control littermates. TRAP, PECAM-1 and Safranin O staining are shown at 10x (left) and 20 x (right) magnifications, with detailed views of the indicated boxes in the bottom row. Note complete absence of TRAP+ osteoclasts in the knock-out mice, unaffected invasion by PECAM-1+ endothelium into the cartilage bone templates, and normal appearance of the perichondrium (bottom, left) and bone collar (bottom), with abundant mesenchymal cells populating the nascent primary ossification center (bottom, right).

(B) Proximal femur of the respective genotypes, stained by Safranin O. The overall structure of the developing bone is similar but RANK-/- mice, lacking osteoclasts completely (TRAP staining, not shown), display increased cartilage remnants in the metaphysis (red stain). The vascularization of the bone is similar in both genotypes (PECAM-1 staining, not shown) and the metaphyseal bone region is populated by osteoblastic cells and peritrabecular stromal cells in both genotypes. These data indicate that the initial cartilage invasion and primary ossification can take place in the absence of osteoclasts in vivo, whereas the further clearance and remodeling of the calcified cartilage into bone requires osteoclasts.

(C) Ex vivo primary ossification center (POC) formation assay. Fully cartilaginous metatarsals dissected from E17.5 embryos (inset; hc, hypertrophic cartilage) cultured with adherence to the recipient surface develop a POC-resembling cavity invaded by PECAM-1+ endothelium. Using metatarsals dissected from Osx-Cre:GFP(Tg/-);Rosa26R(R/-) transgenic embryos, X-gal staining reveals blue cells derived from Osx-expressing cells, several of which can be detected close to the endothelium (PECAM-1 and X-gal staining with magnifications in bottom rows).

(D) Upon blockage of osteoclasts in this culture system by supplementing the culture medium with 50 or 200 ng/ml recombinant OPG the process of POC formation is unaffected and the amount of X-gal staining inside the excavated area is not significantly different from vehicle-treated cultured explants. Bars represent mean ± SEM. See Supplemental Experimental Procedures for details on the quantification methods.

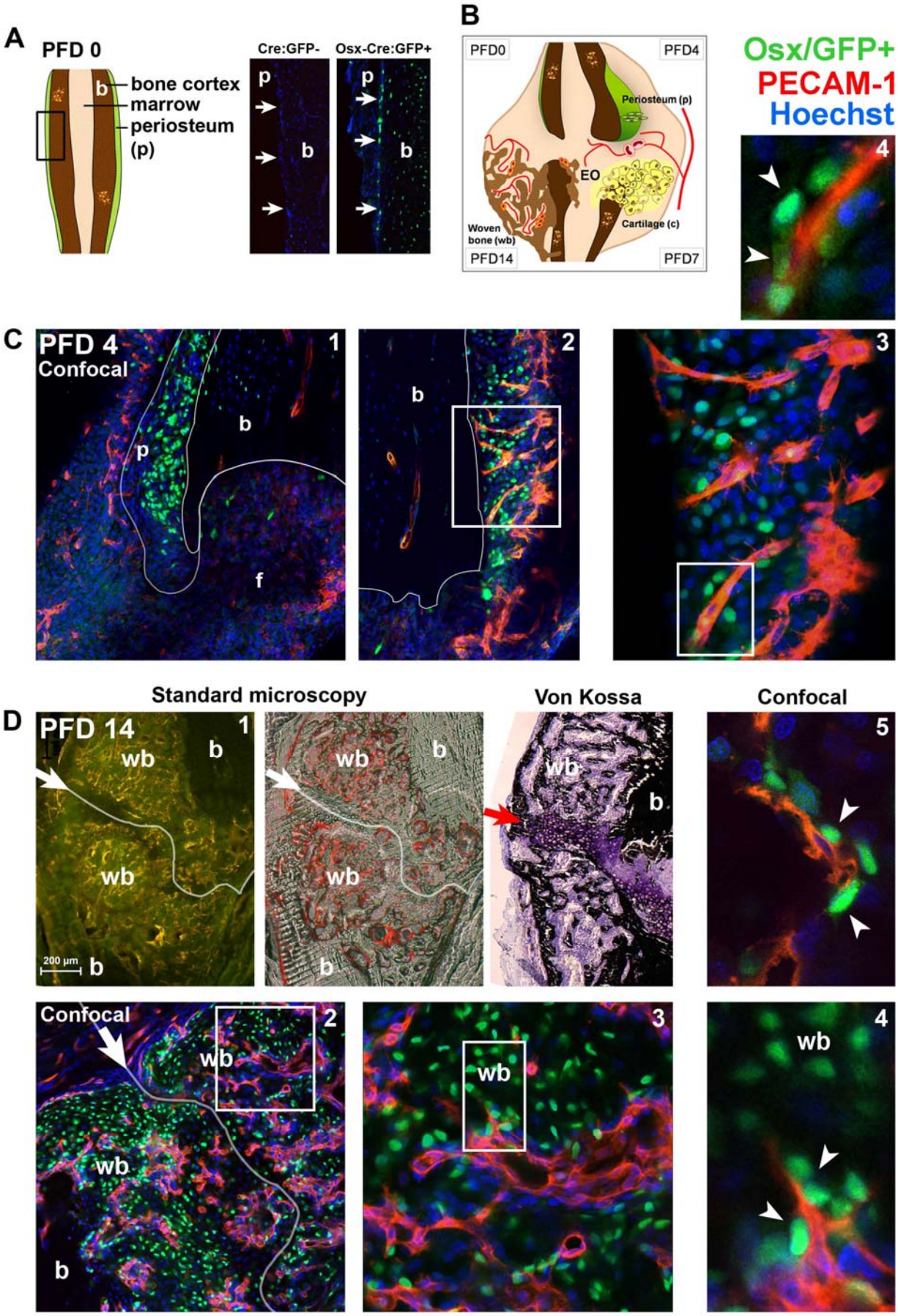

Figure S7. Coupled angiogenesis and osteogenesis in healing fractures is associated with co-localization of Osx-expressing osteoblast lineage cells and blood vessels (related to Figure 7)

(A) Schematical view and histology (single confocal optical slice) of the periosteum (p) (arrows) overlaying the intact cortical bone (b) at post-fracture day 0 (PFD 0) in adult littermates negative (left) or positive (right) for the Osx-Cre:GFP transgene, revealing the presence of Osx/GFP+ cells in the thin periosteal layer of uninjured bones.
(B) Graphical illustration of (clockwise) the subsequent stages of the healing process in the semi-stabilized fracture model analyzed in this study, in which a recapitulated endochondral ossification (EO) process contributes to bone regeneration.
(C) Projections of a set of stacked images taken with a 20x objective (panels 1 and 2) and single slices at 60x (3 and 4, representing progressive magnifications of the boxed areas) by confocal microscopy of PECAM-1 (red, endothelium) and Hoechst (blue, all nuclei) stained sections through the fractured tibia of Osx-Cre:GFP mice at PFD 4. The induction of the bone defect was associated with an early response in the periosteum of the disrupted cortices, with Osx-GFP+ cells being particularly abundant in this thickened periosteum. White lines mark the broken cortical bone ends (b) at the fracture site (f); grey line in (1) points out the contour of the periosteum (p). In periosteal regions that showed vascularization (2-4), affinity of Osx-GFP+ cells for the endothelium was suggested by the frequent co-localization and even immediate juxtaposition (arrowheads in (4)).
(D) Confocal analysis at PFD 14. (1) Overview images taken by standard microscopy at 5x, showing (left-to-right) dark and contrast light views of the analyzed callus section (PECAM-1 signal visible in yellow or red, respectively), and a representative PFD 14 callus plastic section stained by Von Kossa. These images illustrate the abundant woven bone (wb) formed on both sides of the fracture site (arrow and line) at this stage, with only a limited front of remaining fibrous/cartilaginous tissue along the fracture line. (2-5) Confocal analysis of the callus area shown in 1, with increasingly magnified views (3, 4) corresponding to the boxes. Image (5) was captured at a different site in the callus. Osx/GFP+ cells contributed massively to the bony callus, localizing within the woven bone regions (e.g. top part of 4) as well as along the vasculature interspersing the bone fragments (arrowheads in 4 and 5, both representing single optical slices at 60x).
Also see Figure 7 and Movies S1-S4 showing fracture repair data analyzed at PFD 7.

SUPPLEMENTAL EXPERIMENTAL PROCEDURES

Generation and genotyping of transgenic mice

To generate the Osx-CreERt2 and Col1(3.2 kb)-CreERt mouse lines the respective DNA constructs were engineered, purified and injected into the pronucleus of fertilized eggs. Details on the cloning strategy will be made available on request. Briefly, a 200 kb-long BAC clone containing the *Osterix* (*SP7* – Mouse Genome Informatics) gene, RP23-399N14 (BACPAC Resource, CA) was introduced into the recombinogenic bacterial strain EL250 that supports homologous recombination (Lee et al., 2001). To knock-in CreERt2 at the SP7 locus, a mini targeting vector pCS2.FRT-kan.neo (generously provided by Dr. Susan Dymecki, Harvard Medical School) was constructed to contain the CreERt2-encoding cDNA (a kind gift from Dr. Pierre Chambon) (Feil et al., 1996) flanked by two homologous arms to the SP7 gene. The 5' arm was 500 bp long and included the sequence of the

promoter and the first exon up to the translation initiation codon. The vector sequence was released, purified and electroporated into the bacteria carrying the BAC clone. After kanamycin-selection, the homologous recombination was confirmed by PCR, the FRT-kan cassette was removed by flpe expression and residual loxP sequences present in the BAC vector were eliminated by two additional rounds of homologous recombination. For the Col1-CreERt construct, we cloned a CreERt cDNA sequence (Danielian et al., 1998) and poly-A element downstream of a 3.2 kb fragment of the regulatory sequences of the *collagen Iα1* gene (Rossert et al., 1995). Genotyping was done by PCR using PureTaq ready-to-go PCR beads (Amersham Biosciences) or GoTaq Green Master Mix (Promega). Primers for Cre-detection were 5'-CGCGGTCTGGCAGTAAAAACTATC-3' (forward) and 5'-CCCACCGTCAGTACGTGAGATATC-3' (reverse) and Rosa26R primers were as published (Soriano, 1999).

Immunohistochemical staining

Non-fluorescent immunostaining for NG2 was done by incubating paraffin sections with rabbit anti-NG2 antibodies (Chemicon) diluted 1/500 in TNB (NEN, Perkin Elmer) blocking reagent after standard rehydration, quenching (3% H_2O_2 in methanol for 10 min) and blocking (goat antiserum 1/5 in TNB) steps. The secondary goat anti-rabbit antibody (1/300 in TNB) was conjugated with biotin and detected with a streptavidin-HRP complex reacted with DAB (brown). Detection of αSMA included an additional antigen retrieval step by immersing the sections in Tris (10 mmol/l) - EDTA (1 mmol/l) buffer (pH 9.0) for 20 min at 95°C and employed anti-αSMA antibodies at 1/100 dilution (clone 1A4, DAKO). Fluorescent IHC procedures were performed on frozen sections of Osx-Cre:GFP limbs cut at 5 µm, standard including TNB blocking, overnight primary antibody incubation and washes using PBS. Detection of αSMA was direct (1/200 diluted anti-αSMA-Cy3, Sigma), whereas SM22 (1/100; Abcam) was detected with secondary goat anti-rabbit-Cy3 antibodies (1/300 in TNB, 1 h). Mouse anti-desmin monoclonal antibodies (Cappel) were used in combination with the biotinylation Animal Research Kit (DakoCytomation) for use with mouse primary antibodies, and detected with extravidin-Cy3 (1/100 dilution; Sigma). PECAM-1 staining was done as described for DAB-mediated detection on paraffin sections but with use of the fluorescent TSA Cy3 System (NEN) for detection. On thick vibratome sections, an additional pretreatment with proteinase K (10 µg/ml in PBS, 15 min) was performed and TNB was supplemented with 0.1 % Triton X-100. All sections were counterstained with Hoechst nuclear dye and mounted using fluomount medium. Control sections omitting the primary antibodies or replacing with non-specific control IgGs did not show any staining (not shown). Images of the same optic fields were taken using green, red and blue fluorescence filters, and merged by incorporation in the respective channels using Adobe Photoshop software.

In situ hybridization

Detection of Osx (sequence of bases 246-816, accession number AF184902, subcloned to pCRII vector by Mike Burns and Steve Krane, Harvard, Boston), Runx2 and osteocalcin mRNA was done by using radioactive labeled probes as described (Maes et al., 2002). Col1 and osteopontin mRNAs were visualized using DIG-labeled probes according to a modified protocol based on (Tylzanowski et al., 2003). Probes were used at 1/100 dilution and hybridized at 72°C overnight. Detection employed anti-DIG antibodies conjugated with HRP, followed by biotinyl tyramide (NEN) and streptavidin-Alexa568 incubation. Since this procedure abolishes the GFP signal, sections were

imaged prior to ISH. Afterwards, sections were counterstained with Hoechst to visualize the tissue outline and allow perfect matching of pre-ISH and post-ISH images by aligning the nuclear Osx/GFP+ signal with the Hoechst nuclear staining, aided further by inspection and imaging of the slides by contrast light before and after the ISH procedure. When indicated, overlay of (contrast) light and Osx/GFP images is shown to enhance appreciation of the tissue outline. Radioactive ISH signals were captured in white on darkfield images and inserted into the red channel of the corresponding Hoechst images, as done for red fluorescent non-radioactive signals.

FACS sorting, RNA extraction and gene expression analysis by qRT-PCR

Newborn Osx-Cre:GFP mice (n=3 litters) were inspected for the presence of the transgene under fluorescent light and pooled into sample sets of Osx/GFP-negative mice (one pool of 6 mice selected from the three litters) and Osx/GFP+ mice (generating independent pools from each litter with 5-6 pooled animals per sample). Calvaria and the bony parts of the long bones from the limbs and ribs were dissected and digested using 3 mg/ml collagenase and 4 mg dispase in serum-free αMEM for 2-3 hours, shaking at 37°C. Medium containing 10% FCS was added and the isolated cells were filtered through a cell strainer, centrifuged at 1000 rpm for 8 min, washed with PBS, and resuspended at 3.10^6 cells/ml. FACS sorting based on GFP was done on a BD FACSAria Cell Sorter (BD Biosciences). Gates for Osx/GFP+ cell selection (n=4 Osx/GFP+ cell samples retrieved and analyzed for each bone type (calvaria and long bones)) were set based on the negative control samples; the latter were sorted randomly from the basic gated live cell scatter range (FSC/SSC). Pools of 100,000 cells were collected in RLT buffer containing β-mercaptoethanol. RNA was extracted using RNeasy Micro RNA extraction kit (Qiagen) and subjected to cDNA synthesis according to a standard protocol. Real-time qRT-PCR was done on a 7700 Sequence Detector (Perkin Elmer) using 2x PreMix buffer (Applied Biosystems). Primers and probes to quantify HPRT (used as housekeeping gene in all analyses), Runx2, Col1, osteocalcin and VEGF were as before (Maes et al., 2002); the following commercial primer-sets (Applied Biosystems) were used for Osx (Mm00504574_m1), Ang1 (Mm00456498_m1) and PDGFRβ (Mm00435546_n1). Data were analyzed according to the deltaCt method relative to HPRT expression levels.

In vivo and in vitro osteoclast inhibition studies

Limbs were dissected from P0.5 RANK knock-out mice, generously provided by Bill Dougall, Amgen (Dougall et al., 1999), and subjected to paraffin histology as described in the main manuscript Experimental Procedures. Metatarsal cultures were performed according to a modified protocol described before to study angiogenic outgrowth (Deckers et al., 2001). Briefly, fully cartilaginous metatarsals were isolated from E17.5 embryos obtained by timed mating between Osx-Cre:GFP(Tg/-);Rosa26R(R/R) and wild-type CD1 mice, and identified as Osx-Cre:GFP-positive (n=8 embryos used in the experiment) or –negative (n=2) by fluorescence survey. The three middle metatarsals were dissected free and cultured in 24-well plates. The culture medium consisted of αMEM supplemented with 10% FCS and 50 or 200 ng/ml recombinant OPG (Peprotech) and was changed daily. Using small volumes of medium (150 µl during the first three days; 250 µl subsequently) allowed the explants to attach to the recipient surface and develop a sheet of fibroblastic and angiogenic tissue outgrowth as described (Deckers et al., 2001). After 9 days, the samples were washed three times with PBS, fixed for 20 min and stained with X-gal for 3 h at 37°C using solutions described in the X-gal staining procedure. The samples were post-fixed for 2 h in 4%

PFA at 4°C and processed for paraffin histology as described (see Experimental Procedures). Histomorphometry software (AxioVision) was used to define the area of the primary ossification center (POC) formed in vitro, as indicated in Figure S6D (lined area in the SafraninO-stained vehicle section), as well as the relative surface of this area that was occupied with TRAP+ staining (calculating the 'OCL S / POC S (%)', osteoclast surface relative to POC surface) or LacZ+ cells (X-gal surface over POC S (%)) as based on color-selection.

SUPPLEMENTAL REFERENCES

Danielian, P.S., Muccino, D., Rowitch, D.H., Michael, S.K., and McMahon, A.P. (1998). Modification of gene activity in mouse embryos in utero by a tamoxifen-inducible form of Cre recombinase. Curr. Biol. *8*, 1323-1326.

Deckers, M., van der Pluijm, G., Dooijewaard, S., Kroon, M., van Hinsbergh, V., Papapoulos, S., and Lowik, C. (2001). Effect of angiogenic and antiangiogenic compounds on the outgrowth of capillary structures from fetal mouse bone explants. Lab Invest *81*, 5-15.

Dougall, W.C., Glaccum, M., Charrier, K., Rohrbach, K., Brasel, K., De Smedt, T., Daro, E., Smith, J., Tometsko, M.E., Maliszewski, C.R., Armstrong, A., Shen, V., Bain, S., Cosman, D., Anderson, D., Morrissey, P.J., Peschon, J.J., and Schuh, J. (1999). RANK is essential for osteoclast and lymph node development. Genes Dev. *13*, 2412-2424.

Lee, E.C., Yu, D., Martinez de Velasco, J., Tessarollo, L., Swing, D.A., Court, D.L., Jenkins, N.A., and Copeland, N.G. (2001). A highly efficient Escherichia coli-based chromosome engineering system adapted for recombinogenic targeting and subcloning of BAC DNA. Genomics *73*, 56-65.

Rossert, J., Eberspaecher, H., and de Crombrugghe, B. (1995). Separate cis-acting DNA elements of the mouse pro-alpha 1(I) collagen promoter direct expression of reporter genes to different type I collagen-producing cells in transgenic mice. J. Cell Biol. *129*, 1421-1432.

Tylzanowski, P., De Valck, D., Maes, V., Peeters, J., and Luyten, F.P. (2003). Zfhx1a and Zfhx1b mRNAs have non-overlapping expression domains during chick and mouse midgestation limb development. Gene Expr. Patterns. *3*, 39-42.